International Applied Mechanics, Vol. 46, No. 6, 2010

PHOTOELASTIC MODELING OF THE FRACTURE OF VISCOELASTIC ORTHOTROPIC PLATES WITH A CRACK

L. V. Voitovich[1], M. P. Malezhik[1], and I. S. Chernyshenko[2]

The well-known equations of photoelasticity of linear viscoelastic bodies are used to describe the photoelastic behavior of a viscoelastic orthotropic plate with a crack. Expressions for the stress intensity factors (SIFs) at the crack tip are obtained using photoelastic measurements. The time dependence of the SIFs is analyzed and shown to be determined by the angles between directions of the crack and tension

Keywords: photoelasticity, viscoelastic orthotropic plate with a crack, tension, stress intensity, fracture

Introduction. Intensive loading causes early damage of the material of structural members due to the growth of existing and the initiation of new submicro- and microdefects. In many fibrous composites, such processes mainly occur at the fiber–matrix interface. Even at normal temperature, they show viscoelastic behavior [15]. Experimental data [3, 4, 10, 12] suggest that the fracture of such materials largely depends on their rheological properties and may occur at low stresses as a slowly growing crack. Efficient experimental nondestructive methods for the quantitative assessment of the damage of anisotropic materials under loading, especially in the plastic range, are yet to be developed.

Among the direct nondestructive methods that could be used to study the kinetics of damage growth, the acoustic-emission method is the most promising [1]. A review of literature on the use of this method for the evaluation of accumulated damage shows that some well-known data are empirical, which significantly limits their use [14].

The photoelastic method makes it possible to determine stresses and strains and also their distribution in anisotropic optically sensitive materials with accuracy sufficient for engineering [9, 13].

Solutions to nonstationary problems of fracture mechanics for anisotropic bodies with stress concentrators obtained by the dynamic photoelastic method can be found in [17–22, etc.].

We will outline a technique for the determination of the stress intensity factors (SIFs) near cracks in linear viscoelastic materials based on photoelastic measurements. We will discuss results on the variation in the SIFs during precritical crack growth.

1. Problem Formulation and Method of Analysis. Consider a plate made of a linear viscoelastic fibrous composite and having a central crack. The crack is parallel to the direction of preferential reinforcement of the orthotropic composite ($E_1 > E_2$ are the elastic moduli). We choose a rectangular coordinate system x, y with the origin at the crack tip and the Ox-axis aligned with the crack (Fig. 1). The plate is subject to a tensile force P = const. Denote the thickness of the plate by h, the length of the crack by $2l$, and the polar coordinates by r and θ.

To obtain expressions for the stress intensity factors from experimentally found fringe order $m(t)$, we will use the equations of fracture mechanics of viscoelastic bodies [6]. Replacing the elastic constants with creep functions $\psi_{ij}(t)$, we obtain formulas for the stresses $\sigma_{xx}, \sigma_{yy}, \tau_{xy}$ at the crack tip:

$$\sigma_{xx} = \{K_I(t)\xi_1(t)\xi_2(t)[\xi_2(t)n_2(t) - \xi_1(t)n_1(t)]/A(r,t)\}$$

[1]M. P. Dragomanov National Pedagogical University, 9 Pirogov St., Kyiv, Ukraine 01601, e-mail: malez@ukr.net.
[2]S. P. Timoshenko Institute of Mechanics, National Academy of Sciences of Ukraine, 3 Nesterov St., Kyiv, Ukraine 03057, e-mail: prikl@inmech.kiev.ua. Translated from Prikladnaya Mekhanika, Vol. 46, No. 6, pp. 76–82, June 2010. Original article submitted July 2, 2009.

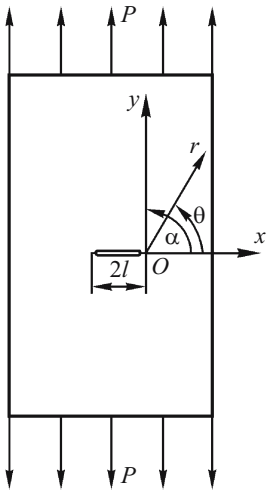

Fig. 1

$$+\{K_{\mathrm{II}}[\xi_1^2(t)p_1(t)-\xi_2^2(t)p_2(t)]/A(r,t)\}+\sigma_{Ox},$$

$$\sigma_{yy}=\{K_{\mathrm{I}}(t)\xi_1(t)[\xi_2(t)n_1(t)-\xi_1(t)n_2(t)]/A(r,t)\}+\{K_{\mathrm{II}}[p_2(t)-p_1(t)]/A(r,t)\},$$

$$\tau_{xy}=K_{\mathrm{I}}(t)\xi_1(t)\xi_2(t)[p_1(t)-p_2(t)]/A(r,t)+K_{\mathrm{II}}(t)[\xi_2(t)n_2(t)-\xi_1(t)n_2(t)]/A(r,t), \tag{1}$$

where $K_{\mathrm{I}}=\sigma_0\sin^2\alpha[\pi l(t)]^{1/2}$ and $K_{\mathrm{II}}=\sigma_0\sin\alpha\cos\alpha[\pi l(t)]^{1/2}$ are the stress intensity factors; σ_{Ox} are far-field stresses;

$$n_j(t)=\frac{1}{\sqrt{\upsilon_j}}\cos\frac{\gamma_j}{2},\qquad p_j=\frac{1}{\sqrt{\upsilon_j}}\sin\frac{\gamma_j}{2},\qquad \tan\gamma_j=\xi_j(t)\tan\theta,\qquad \upsilon_j(t)=\sqrt{\cos^2\theta+\xi_j^2(t)\sin^2\theta},$$

$$A(r,t)=\sqrt{2\pi}[\xi_2(t)-\xi_1(t)],\qquad i\xi_j(t)=\mu_j(t),\qquad -i\bar{\xi}_j(t)=\bar{\mu}_j(t)\qquad (j=1,2),$$

$\mu_j(t)$ are complex parameters corresponding to the complex conjugate roots of the following characteristic equation [7]:

$$\mu^4(t)+[2\psi_{12}(t)+\psi_{66}(t)]/\psi_{11}(t)\mu^2(t)+\psi_{22}(t)/\psi_{11}(t)=0. \tag{2}$$

As in [12], we write the photoviscoelastic equations in quasielastic approximation [13]:

$$\left[\frac{m(t)}{h}\right]^2=\Big\{\cos^2\theta[F_{11}(t)\sigma_{xx}(t)-F_{22}(t)\sigma_{yy}(t)]+\sin^2\theta\Big[F_{11}(t)\sigma_{yy}(t)-F_{22}(t)\sigma_{xx}(t)\Big]$$

$$+\sin 2\theta[F_{11}(t)+F_{22}(t)]\tau_{xy}(t)\Big\}+\{\sin 2\theta F_{12}(t)[\sigma_{xx}(t)-\sigma_{yy}(t)]-2\cos 2\theta F_{12}(t)\tau_{xy}(t)\}^2, \tag{3}$$

where $F_{ij}(t)$ is the optical creep function.

If the plate is stretched at angle $\alpha=90°$ to the crack, and the fringe order $m(t)$ is measured along the polar radius r drawn from the crack tip at angle $\theta=90°$ (Fig. 1), Eqs. (1) with (3) become

$$\sigma_{xx}(t)=\frac{K_{\mathrm{I}}(t)}{2\sqrt{\pi r}}\frac{\xi_1(t)\xi_2(t)}{\sqrt{\xi_1(t)}+\sqrt{\xi_2(t)}}+\sigma_{0x},\qquad \sigma_{yy}(t)=\frac{K_{\mathrm{I}}(t)}{2\sqrt{\pi r}}\frac{b(t)}{c(t)\xi_1(t)\xi_2(t)},$$

$$\tau_{xy}(t)=\frac{K_{\mathrm{I}}(t)}{2\sqrt{\pi r}}\frac{[\xi_1(t)\xi_2(t)]^{1/2}}{a(t)}, \tag{4}$$

TABLE 1

$\psi_{ij}, \xi_{ij}, F_{ij}$	t, min						
	0	10	20	30	40	50	60
$\psi_{11}(t)$	2.42	2.48	2.57	2.65	2.71	2.75	2.77
$\psi_{22}(t)$	3.76	3.88	4.10	4.29	4.33	4.40	4.49
$\psi_{12}(t)$	–1.02	–1.06	–1.10	–1.14	–1.16	–1.18	–1.21
$\psi_{66}(t)$	11.98	12.71	13.51	14.12	14.63	15.16	15.51
$\xi_1(t)$	1.89	1.93	1.98	2.00	2.08	2.09	2.10
$\xi_2(t)$	0.67	0.65	0.64	0.63	O.63	0.62	0.61
$F_{11}(t)$	0.62	0.63	0.64	0.65	0.65	0.65	0.65
$F_{22}(t)$	0.83	0.86	0.89	0.91	0.93	0.94	0.94
$F_{12}(t)$	0.88	0.94	0.97	0.99	1.00	1.03	1.04

where $a(t)=\xi_2^{1/2}(t)-\xi_1^{1/2}(t)$, $b(t)=\xi_1^2(t)+\xi_1(t)\xi_2(t)+\xi_2^2(t)$, $c(t)=\xi_2^{3/2}(t)+\xi_1^{3/2}(t)$.

Then Eqs. (3) with (4) take the form

$$[m(t)/h]^2=[F_{11}(t)\sigma_{yy}(t)-F_{22}(t)\sigma_{xx}(t)]^2+4F_{12}^2(t)\tau_{xy}^2(t). \tag{5}$$

Substituting expressions (4) into (5), we obtain an equation relating the fringe order $m(t)$ with K_I and σ_{Ox}:

$$[(m(t)/h]^2=\frac{K_{\mathrm{I}}^2(t)}{4\pi r}\Big\{F_{11}^2(t)b(t)/c^2(t)\xi_1(t)\xi_2(t)+F_{22}^2(t)\big[\xi_1(t)\xi_2(t)\big]^2/a^2(t)$$

$$+4F_{12}^2(t)\xi_1(t)\xi_2(t)/a^2(t)-2F_{11}(t)F_{22}(t)b(t)[\xi_1(t)\xi_2(t)]^{1/2}/a(t)c(t)\Big\}$$

$$+\frac{K_{\mathrm{I}}(T)\sigma_{Ox}}{2\sqrt{\pi r}}\{\xi_1(t)\xi_2(t)/a(t)+b(t)/c(t)[\xi_1(t)\xi_2(t)]^2\}+F_{22}^2(t)\sigma_{Ox}^2. \tag{6}$$

If the plate is stretched at angle $\alpha=45°$ to the crack, and the fringe order $m(t)$ is measured along the radius drawn from the crack tip at angle $\theta=0°$, expressions (1) and (3) become

$$\sigma_{xx}(t)=\frac{K_{\mathrm{I}}(t)}{\sqrt{2\pi r}}\xi_1(t)\xi_2(t)+\sigma_{Ox},\qquad \sigma_{yy}(t)=\frac{K_{\mathrm{I}}(t)}{\sqrt{2\pi r}},\qquad \tau_{xy}(t)=\frac{K_{\mathrm{II}}(t)}{\sqrt{2\pi r}}, \tag{7}$$

$$[m(t)/h]^2=[F_{11}(t)\sigma_{xx}(t)-F_{22}(t)\sigma_{yy}(t)]^2+4F_{12}^2(t)\tau_{xy}^2(t). \tag{8}$$

Equations (7) and (8) yield the following equation relating $m(t)$ and $K_{\mathrm{I}}, K_{\mathrm{II}}, \sigma_{Ox}$ for the case of load being considered:

$$[m(t)/h]^2=K_{\mathrm{I}}^2(t)\{F_{11}^2(t)[\xi_1(t)\xi_2(t)]^2+F_{22}^2(t)-2F_{11}(t)\xi_1(t)\xi_2(t)\}/2\pi r$$

$$+K_{\mathrm{II}}^2(t)2F_{12}^2(t)/\pi r+K_{\mathrm{I}}(t)\sigma_{Ox}[2F_{11}^2(t)\xi_1(t)\xi_2(t)-2F_{11}(t)F_{22}(t)]/\sqrt{2\pi r}+F_{11}^2(t)\sigma_{Ox}^2. \tag{9}$$

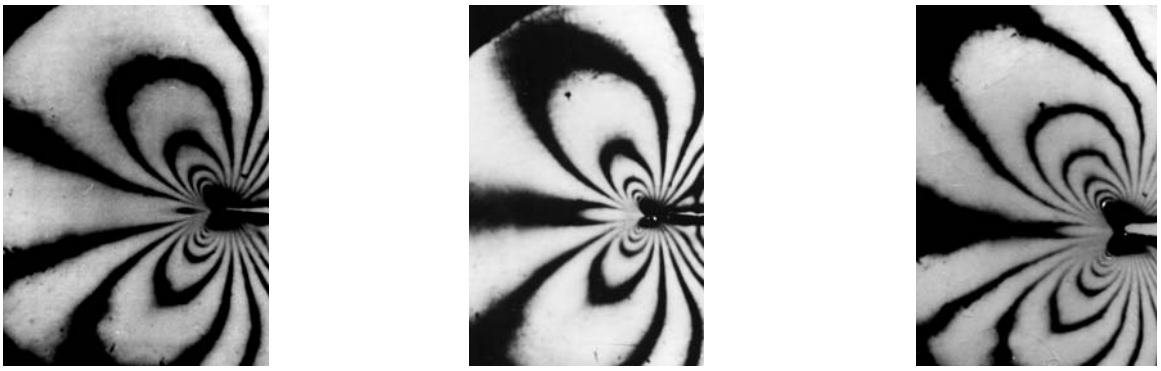

Fig. 2

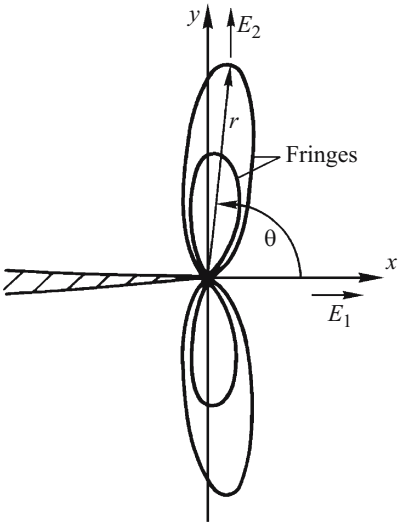

Fig. 3

Hence, Eqs. (6), (9) and known values of the fringe order $m(t)$ can be used to determine K_{I}, K_{II} and to analyze their variation with time.

2. Experimental Data and Their Analysis. To determine the SIFs by the photoelastic method, we tested plates made of composite with ED-16 epoxy matrix (100 wt%) cured with polyethylenepolyamine (12 wt%) and plasticized with polyesters (10 wt%). The manufacturing technique for the this photoelastic material is well-known [11]. To study the mechanical and optical properties of materials, we used dumb-bell test pieces (as per GOST 11262-80 Soviet Standard) cut from plates along the principal reinforcement directions $\theta = 0°$, $\theta = 90°$ and at angle $\theta = 45°$. The specimens were stretched to creep. Deformation was measured and recorded with a rosette of two orthogonal foil strain gages and KST-4 strain gage bridge. Changes in the fringe order were recorded with a KSP-10 coordinate-synchronized polarimeter. The known strains $\varepsilon_1(t)$, $\varepsilon_2(t)$ and the tensile forces were used to determine the creep functions $\psi_{ij}(t)$ and then the complex parameters $\mu_j(t)$ from Eq. (2). In much the same way, the fringe order $m(t)$ and tensile forces were used to determined the optical creep function $F_{ij}(t)$ by the well-known technique [12].

Table 1 summarizes the values of the functions $\psi_{ij}(t)\cdot 10^{-4}$ MPa^{-1}, parameters $\xi_j(t)$ $(j = 1, 2)$, and functions $F_{ij}(t)$, fringe/MPa·cm at some time points $(t = 0, \ldots, 60)$.

The test plates $(E_1 > E_2)$ had a thickness of 2.5 mm, a width of 55 mm, and a length of 200 mm. Cracks 0.15 mm wide and $2l = 7$ mm long were made by notching. The plate was stretched at angle $\alpha = 90°$ to the crack by uniform load $P = 860$ N. The coordinates of fringes along the radius r drawn from the crack tip at angle $\alpha = 90°$ (Fig. 3) were determined at certain time intervals from the isochromatic pattern (Fig. 2) in the KSP-10 polarimeter and used to plot the distribution of fringe orders

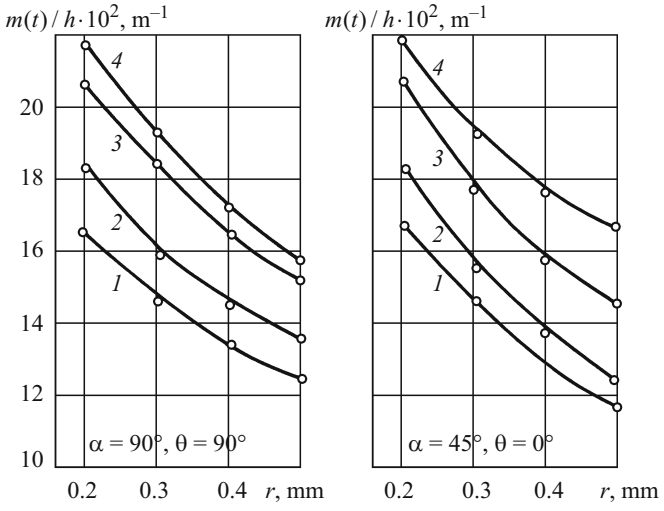

a *b*

Fig. 4

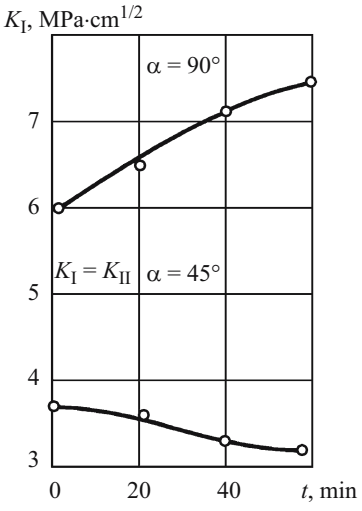

Fig. 5

$m = \varphi(r)$ (Fig. 4). Figures 4*a* and 4*b* represent the cases of tension at angle $\alpha = 90°$ ($\theta = 90°$) and $\alpha = 45°$ ($\theta = 0°$), respectively. Lines *1–4* correspond to $t = 0$, 10, 30, 60 min.

The fringe order $m(t)$ was determined by the de Senarmont compensation method for two wavelengths $\lambda_1 = 0.456 \cdot 10^{-6}$ m and $\lambda_2 = 0.578 \cdot 10^{-6}$ m. The error of such measurements did not exceed 4% [5].

The plate was stretched at angle $\alpha = 45°$ to the crack by uniform force P = 990 N. As in the previous case, the coordinates of the fringes along the radius emerging from the crack tip at angle $\theta = 0°$ (Fig. 4*b*) were determined. Equation (6) and the known values of m and r were used to find $K_I(t)$ for $t = 0$, 10, 30, 60 min (Fig. 5). The stress intensity factors $K_I(t)$ and $K_{II}(t)$ at these time points were determined using Eq. (9). The nonlinear equations (6) and (9) were solved by the Newton–Raphson method in combination with the least-squares method [8].

The variation in $K_I(t)$ and $K_{II}(t)$ is shown in Fig. 5 for two cases of tension ($\alpha = 90°$, 45°).

An analysis of the fracture surface photographs of the viscoelastic plate shows that slow precritical crack growth in the composite is accompanied by the formation and growth of a long wedge-shaped fracture process zone located at the crack tip and extended along the continuation of the crack. This zone includes damaged fibers, and its edges are restrained by undamaged fibers. Note that similar results were obtained in [3]. This fracture pattern is similar to that observed in linear polymers where the structure of process zones is similar to a craze [16].

The data reported here confirm the theoretical results on precritical crack growth obtained with the RS-model in fracture mesomechanics [2, 3] and take into account (within the framework of a linear formulation) the viscoelastic properties of the matrix and fibers in the fracture process zone.

Conclusions. Experimental data for viscoelastic plates with a crack under tension show that the stress intensity factors vary with time and that this time dependence is strongly affected by the angle α between the directions of the crack and tension. The factor $K_I(t)$ increases with time when $\alpha = 90°$, whereas $K_I(t)$ and $K_{II}(t)$ slightly decrease when $\alpha = 45°$.

The developed technique for the determination of the SIFs at a crack based on optical measurements and the results obtained can be used in designing load-bearing structural memebers made of polymeric fibrous materials and resisting long-term static loads. Photoelastic modeling of the mechanical behavior of orthotropic viscoelastic structures with crack-like concentrators makes it possible to predict their service life and is a promising area in the fracture mechanics of anisotropic materials.

REFERENCES

1. O. E. Andreikiv, V. R. Skal'skii, and O. M. Sergienko, "Acoustic emission criteria for the express-evaluation of internal damage of composite materials," *Fiz.-Khim. Mekh. Mater*., No. 2, 84–92 (2003).
2. A. A. Kaminsky, "Rheological structural model of a crack in a viscoelastic composite material," *Int. Appl. Mech*., **28**, No. 7, 415–420 (1992).
3. A. A. Kaminsky and D. A. Gavrilov, *Long-Term Fracture of Polymeric and Composite Materials with Cracks* [in Russian], Naukova Dumka, Kyiv (1992).
4. A. A. Kaminsky and M. F. Selivanov, "Long-term failure of a layered viscoelastic composite material with a crack under a time-dependent load," *Mech. Comp. Mater*., **36**, No. 4, 327–336 (2000).
5. E. I. Edel'shtein, M. V. Leikin, N. M. Drichko, et al., "Coordinate-synchronized polarimeter KSP-10," in: *Proc. 8th All-Union Conf. on the Photoelastic Method* [in Russian], Vol. 2, Tallinn (1979), pp. 77–84.
6. H. T. Corten, "Fracture mechanics of composites," in: H. Liebowitz (ed.), *Fracture: An Advanced Treatise*, Vol. 7, Acad. Press, New York (1972), pp. 695–703.
7. S. G. Lekhnitskii, *Anisotropic Plates*, Gordon and Breach, New York (1968).
8. I. I. Lyashko, V. L. Makarov, and A. K. Skorobagat'ko, *Computing Techniques* [in Russian], Vyshcha Shkola, Kyiv (1977).
9. M. P. Malezhik, *Dynamic Photoelasticity of Anisotropic Bodies* [in Ukrainian], IGF NAN Ukrainy im. Subbotina, Kyiv (2001).
10. M. P. Malezhik, "Modeling the stress–strain state near cracks in anisotropic linear viscoelastic plates," *Fiz.-Khim. Mekh. Mater*., No. 2, 93–95 (2003).
11. M. P. Malezhik, "Optically sensitive materials for modeling stress wave fields in anisotropic bodies," *Fiz.-Khim. Mekh. Mater*., No. 1, 99–103 (2004).
12. M. P. Malezhik and O. P. Malezhik, "Determining the stress intensity factors for viscoelastic anisotropic plates with a crack subject to long-term fracture," *Nauk. Visti NTTU "KPI*," No. 3, 70–74 (2005).
13. V. P. Netrebko and I. P. Vasil'chenko, *Polarization Methods in the Mechanics of Composite Materials* [in Russian], Izd. Mosk. Univ., Moscow (1990).
14. V. R. Skal's'kyi, "Acoustic-emission analysis of accumulated bulk damage in solids," *Fiz.-Khim. Mekh. Mater*., No. 1, 91–100 (2001).
15. A. M. Skudra, F. Ya. Bulavs, and K. A. Rotsens, *Creep and Static Fatigue of Reinforced Plastics* [in Russian], Zinatne, Riga (1971).
16. M. I. Shut and N. M. Zazimko, "Studying the initiation and growth of a main crack," in: *Trans. M. P. Dragomanov National Pedagogical University* [in Ukrainian], issue 2, NPU, Kyiv (2001), pp. 3–8.
17. M. P. Malezhik and I. S. Chernyshenko, "Solution of nonstationary problems in the mechanics of anisotropic bodies by the method of dynamic photoelasticity," *Int. Appl. Mech*., **45**, No. 9, 954–980 (2009).
18. M. P. Malezhik, I. S. Chernyshenko, and G. P. Sheremet, "Photoelastic simulation of the stress wave field around a tunnel in an anisotropic rock mass subject to shock load," *Int. Appl. Mech*., **42**, No. 8, 948–950 (2006).
19. M. P. Malezhik, I. S. Chernyshenko, and G. P. Sheremet, "Diffraction of stress waves by a free or reinforced hole in an orthotropic plate," *Int. Appl. Mech*., **43**, No. 7, 767–772 (2007).
20. M. P. Malezhik, O. P. Malezhik, and I. S. Chernyshenko, "Photoelastic determination of dynamic crack-tip stresses in an anisotropic plate," *Int. Appl. Mech*., **42**, No. 5, 574–581 (2006).
21. M. P. Malezhik, O. P. Malezhik, A. I. Zirka, and I. S. Chernyshenko, "Dynamic photoelastic study of wave fields in elastic plates with stress concentrators," *Int. Appl. Mech*., **41**, No. 12, 1399–1406 (2005).
22. M. P. Malezhik, O. P. Malezhik, A. I. Zirka, and I. S. Chernyshenko, "Stress wave fields in plates weakened by curvilinear holes with edge cracks," *Int. Appl. Mech*., **42**, No. 2, 192–195 (2006).